Generation of minimally persistent circle formation for a multi-agent system*

Luo Xiao-Yuan(罗小元)[a], Shao Shi-Kai(邵士凯)[a], Zhang Yu-Yan(张玉燕)[a], Li Shao-Bao(李绍宝)[b], Guan Xin-Ping(关新平)[a], and Liu Zhi-Xin(刘志新)[a]†

[a] School of Electrical Engineering, Yanshan University, Qinhuangdao 066004, China
[b] Department of Mechanical and Biomedical Engineering, City University of Hong Kong, Kowloon, Hong Kong, China

(Received 13 January 2013; revised manuscript received 10 July 2013; published online 10 December 2013)

In this paper, two methods of generating minimally persistent circle formation are presented. The proposed methods adopt a leader-follower strategy and all followers are firstly motivated to move into the leader's interaction range. Based on the information about relative angle and relative distance, two numbering schemes are proposed to generate minimally persistent circle formation. Distributed control laws are also designed to maintain the desired relative distance between agents. The distinctive features of the proposed methods are as follows. First, only $2n-3$ unilateral communication links for n agents are needed during the circle formation process and thus the communication complexity can be reduced. In addition, the formation topology is kept fixed for the whole motion and achieves a self-stability property. Finally, each follower keeps a regualr interval with its neighbors and the formation converges to a uniform circle formation. Simulation results are also provided to demonstrate the effectiveness of the proposed methods.

Keywords: multiagent system, formation control, minimally persistent graph, numbering strategy

PACS: 89.20.Ff, 87.85.St, 89.65.Ef, 02.30.Em **DOI:** 10.1088/1674-1056/23/2/028901

1. Introduction

In recent years, there has been considerable interest in the area of multi-agent systems (MASs).[1–5] These systems can potentially consist of a great number of agents, such as unmanned aerial vehicles (UAVs), unmanned ground vehicles (UGVs), and unmanned underwater vehicles (UUVs). MASs are found to have numerous applications in various practical fields,[6,7] such as in terrestrial, space, or oceanic exploration, enhancing the efficiency of surveillance and rescue missions, or even contributing to the development of automated transportation systems.[8,9] The advantages of MASs over single agent include cost reduction, efficiency, and robustness improvement, etc.

One interesting issue of multi-agent system is formation control. Its objective is to design algorithms to motivate agents to form a desired formation. Rigid formation and persistent formation are two important configurations.[10–12] In the rigid formation and persistent formation, configurations can be maintained consistently if all interaction edges are kept. A rigid formation is a kind of undirected configuration while a persistent formation is directed configuration related to one rigid formation. Many scholars have studied the decreasing of communication complexity based on rigid and persistent configurations.[13–15] In Ref. [16], the authors have studied minimally persistent formation, a kind of persistent formation with the least communication number was proposed, but what they focused on was the generation process and they did not study its application in formation shape control.

Recently, many researchers have studied the formation shape control problem.[17–19] The basis for shape control is to design controllers that can maintain a desired distance between communicating agents. Shape control for circle formation is an important issue in MASs. A circle formation system can be used to imitate animal predation or to execute a pursuit-evasion game. In the wireless sensor network coverage area, a circle formation consisting of several mobile sensors can be viewed as the basic component to cover the target area. Lots of researchers have focused on circle formation control and target-enclosing problem.[20–23] In Ref. [20], control laws for moving-target-enclosing were designed and the control laws were composed of two parts, aiming to keep the desired distance between the target and the neighbors. In Ref. [21], a virtual agent was first introduced, then control laws based on consensus algorithm were designed. In Ref. [22], multi-target pursuit formation was considered and the state information of angles was used to control the motion of all agents. In Refs. [20]– [23], the authors all assumed that every follower can obtain the target state information by itself, which may be impractical in many cases considering the limited interaction range of each agent. Besides, the authors mainly studied the complicated control laws and scarcely took the topology generation for circle formation into account, which, in fact, may play an important role in generating the circle formation.

*Project supported by the National Basic Research Program of China (Grant No. 2010CB731800), the National Natural Science Foundation of China (Grant Nos. 60934003, 61074065, and 61375105), and the Natural Science Foundation of Hebei Province, China (Grant No. F2012203119).

†Corresponding author. E-mail: lzxauto@ysu.edu.cn

© 2014 Chinese Physical Society and IOP Publishing Ltd

In this paper, we mainly concentrate on topology generation and have developed a novel framework for circle formation control. Compared with the methods in Refs. [20]–[23], the method in this paper is easy and straightforward. Our two main contributions are constructing minimally persistent configurations with only $2n-3$ unilateral communication links and designing controllers to maintain the desired distances between agents. The leader-follower approach and limited interaction range of each agent are considered in this paper. Firstly, two types of followers are considered at an initial time instant. Controllers for each agent are designed which can motivate all followers to move into the leader's interaction range. Then, two numbering strategies are presented to generate minimally persistent topology, thus breaking up the initial state assumptions of agents in Refs. [20] and [21] and reducing communication complexity. Besides, the numbering strategies are applicable for any formation system, no matter whether the agent number is even or odd, and show good validity, even when some followers of the system are broken down. Finally, distributed control laws are designed to maintain the desired relative distances between agents. The topology of the system is kept fixed for the whole following motion, and a self-stability property is possessed by the system. Each follower ultimately converges to a position to keep a regular interval from its neighbors and a uniform circle formation is generated.

2. Preliminaries and problem formulation

2.1. Graph theory

A graph G consists of a vertex set $V=\{1,2,\ldots,n\}$ and an edge set $E\subset V\times V$, where each edge $e\subset E$ is a pair of vertices (i,j), such that $i\neq j$. For a graph G with $\forall(i,j)\in E$, if we can deduce $(j,i)\in E$, then graph G is an undirected graph. For a graph G, if $\forall(i,j)\in E$ is an ordered pair of distinct vertices i,j, which is that $\forall(i,j)\in E$ does not mean $(j,i)\in E$, then we say that the graph G is a directed graph. In this graph, vertices of the graph represent agents in the formation. For a directed graph, the directed edges represent the unilateral communication. In this paper, the directed edge $(\boldsymbol{i},\boldsymbol{j})$ means that agent i can sense agent j through its sensor and locate its relative position or measure the distance.

A rigid graph is a type of undirected graph and means that all the inter-agent distances remain constant during a continuous displacement. A persistent graph has the same characteristic of maintaining the constant inter-agent distances, but it is a directed graph. A persistent graph can be obtained from a relevant rigid graph by adding directions on all edges, but we cannot generate a persistent graph by adding arbitrary directions on the edges. The out-degree of each vertex should be no larger than two if we want to obtain the persistent graph.[15] Besides, rigid graphs and persistent graphs are not unique.

In this paper, minimally rigid graphs and minimally persistent graphs are two important notions. A minimally rigid graph is a rigid graph such that no edge can be removed without losing rigidity.[16] A minimally persistent graph is somewhat similar to the minimally rigid graph. The definition of minimally persistent graph is given as follows.

Definition 1[14] In R^2, a graph is minimally persistent graph if its underlying undirected graph is a minimally rigid graph and the out-degree of each vertex is no larger than two.

From Ref. [16] it follows that an n-vertex minimally rigid graph has $2n-3$ undirected edges. So, according to Definition 1, a minimally persistent graph has $2n-3$ directed edges. Figure 1 shows an example of minimally persistent graph, where what figure 1(a) shows is not a minimally persistent graph since the out-degree of x_3 is three; figure 1(b) shows a persistent graph but not a minimally persistent graph; figure 1(c) displays a minimally persistent graph.

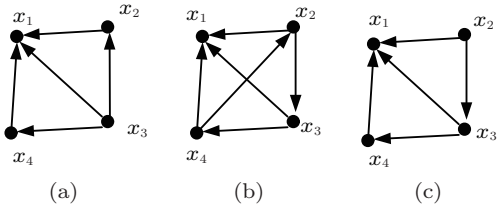


Fig. 1. Examples of minimally persistent graph.

Now, we introduce the notions of collinear and non-collinear formations. Collinear and non-collinear formations are applied only to systems with more than two agents. Intuitively, if three or more agents are dispersed in a line, then they are said to be collinear, otherwise they are non-collinear.

In this paper, the formation control problem of multi-agent systems is based on graph theory. All agents are denoted by vertices and all interactions are denoted by edges between vertices.

2.2. System modeling and problem formulation

Multi-agent systems Define a set of agents as $\Omega=\{i:i=1,2,\ldots,n\}$, where n is the number of agents. For agent i in a two-dimensional coordinate, the position and input vectors are denoted by $p_i\in R^2$ and $u_i\in R^2$, respectively. The dynamics of agent i at time t are described by the following continuous-time equation:

$$\dot{p}_i(t)=u_i(t). \tag{1}$$

Each agent can only obtain the state information of its neighbors. The neighboring set of agent i is denoted as

$$N_i(t)=\left\{j:\|p_i-p_j\|<r,j\in(1,2,\ldots,n),j\neq i\right\}, \tag{2}$$

where $r>0$ denotes the maximum interaction range of every agent.

In this paper, all of the maximum interaction ranges of agents are assumed to be an identical limited value. For the formation system, only one leader is considered and all the others are followers. The agent that has the most neighbors is chosen as the leader. The followers are assumed as follows.

Part of the followers can sense the leader and are called the α-type followers, and denoted as $\Omega_\alpha = \{1, 2, \ldots, n_\alpha\}$. The others that cannot sense the leader are called the β-type followers, and each of them is assumed in the interaction range of at least one α-type follower, which is for analysis simplicity. These β-type followers are denoted as $\Omega_\beta = \{1, 2, \ldots, n_\beta\}$. Figure 2 shows two types of followers. In Fig. 2, r is the interaction radius of each agent. The real circle denotes the leader's interaction range. The dashed circle denotes the interaction range of one β-type follower. All α-type followers are within the leader's interaction range. Each β-type follower can sense at least one α-type follower.

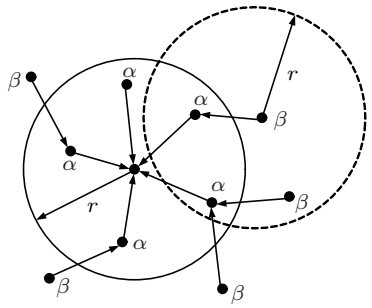


Fig. 2. Example of α-type and β-type followers.

Remark 1 The reason why we consider different types of followers is that taking sensor's interaction range into account is meaningful in practical cases. Meanwhile, we mainly concentrate on topology generation. In order to simplify the motion process, each β-type follower is considered to be able to sense at least one α-type follower. As assumed, the model opens a new perspective to make agents move into the leader's interaction range without directly sensing the leader.

In the following, the leader-follower approach is adopted for the formation control problem. All of the agents are assumed to move initially with a constant velocity v_0. Two numbering strategies and agent controllers are designed to motivate all followers to generate a uniform circle formation.

3. Circle formation for multi-agent systems

In this section, two numbering strategies are proposed and the corresponding controllers to maintain relative distances between agents are designed. Firstly, control laws for β-type followers are designed to motivate these followers to move into leader's interaction range. Then, all of the agents are controlled to form a uniform circle formation by the two strategies and the designed controllers.

3.1. Control laws for β-type followers

At the initial time instant, all agents move in the workplace with a constant velocity v_0. In order to form the desired formation, controllers to make all β-type followers move into leader's interaction range are first designed.

Since each β-type follower is within the interaction range of at least one α-type follower, dynamic controllers for the formation are designed as follows:

$$u_{\mathrm{L}} = v_0; \tag{3}$$

$$u_{\alpha i} = v_0, \quad i \in \Omega_\alpha; \tag{4}$$

$$u_{\beta j} = v_0 + k_1 \left(p^*_{\alpha j} - p_{\beta j} - \frac{p^*_{\alpha j} - p_{\beta j}}{\| p^*_{\alpha j} - p_{\beta j} \|} r^* \right), \quad k_1 > 0, j \in \Omega_\beta; \tag{5}$$

where u_{L} and $u_{\alpha i}$ are the inputs for the leader and α-type followers, respectively; $u_{\beta j}$ is the input of the j-th β-type follower; $k_1 > 0$ is a constant; $p^*_{\alpha j}$ denotes the position information of the nearest α-type follower of the j-th β-type follower; and, $r^* > 0$ represents the safe distance between any two agents.

Theorem 1 Assume that all agents governed by Eq. (1) are controlled by Eqs. (3)–(5), then all β-type followers will move to maintain the safe distance from its nearest α-type followers.

Proof Considering a β-type follower and its nearest α-type follower, one has

$$\begin{aligned} & \dot{p}_{\beta j}(t) - \dot{p}^*_{\alpha j}(t) \\ = \; & u_{\beta j}(t) - u^*_{\alpha j}(t) \\ = \; & k_1 \left(p^*_{\alpha j}(t) - p_{\beta j}(t) - \frac{p^*_{\alpha j}(t) - p_{\beta j}(t)}{\| p^*_{\alpha j}(t) - p_{\beta j}(t) \|} r^* \right). \end{aligned} \tag{6}$$

At arbitrary time instant, $p^*_{\alpha j}(t)$ can be considered as a constant. Therefore, one can deduce from Eq. (6) that

$$p_{\beta j}(t) - p^*_{\alpha j}(t) = \left(C_1 \mathrm{e}^{-k_1 t} - r^* \right) \frac{p^*_{\alpha j}(t) - p_{\beta j}(t)}{\| p^*_{\alpha j}(t) - p_{\beta j}(t) \|}, \tag{7}$$

where C_1 is a constant.

From Eq. (7), one can find that $\| p_{\beta j}(t) - p^*_{\alpha j}(t) \| = r^*$ when $t \to \infty$, which means that the β-type follower would maintain the safe distance from its nearest α-type follower. Then, deduced by analogy, all β-type followers will keep the safe distance from their nearest α-type followers. Theorem 1 is proved.

Now, we come to consider the following problem by taking the leader into account. There are two cases as shown in Fig. 3, where the solid line circle denotes the leader's maximum interaction range; the radius of the dashed line circle is the safe distance. In Fig. 3(a), point β' is the final position; in Fig. 3(b), point β' is the intermediary position and point β'' is the final position.

a) The β-type followers have already moved into the leader's interaction range before they keep a safe distance from the corresponding α-type one, as shown in Fig. 3(a).

b) The β-type followers do not move into the leader's interaction range when they have already achieved a safe distance, as shown in Fig. 3(b).

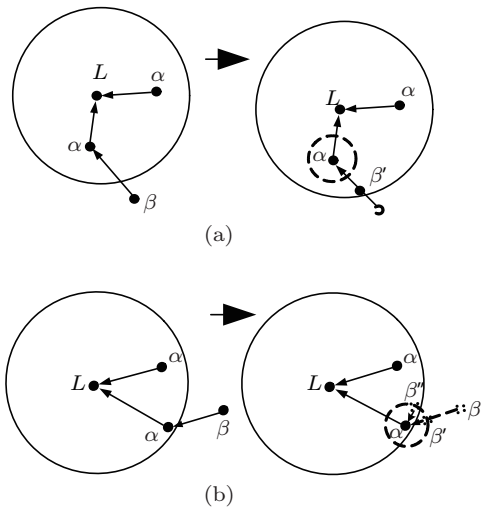


Fig. 3. Two cases for β-type followers.

The control strategies for β-type followers are as follows. First, all β-type followers are driven by Eq. (5) to move toward their corresponding nearest α-type ones. For the first case, the β-type follower stops moving when it can sense the leader. For the second case, the β-type follower keeps moving under Eq. (5) until it achieves a safe distance from the nearest α-type one, then the β-type follower is driven by the following controller:

$$\begin{aligned}\overline{u}_{\beta j} &= v_0 + k_1\left(p^*_{\alpha j} - p_{\beta j} - \frac{p^*_{\alpha j} - p_{\beta j}}{\|p^*_{\alpha j} - p_{\beta j}\|} r^*\right) \\ &\quad + \frac{k_1}{2}\boldsymbol{a}, \quad j \in \Omega_\beta, \end{aligned} \tag{8}$$

where k_1 is a positive constant and $\boldsymbol{a} = [p^*_{jy} - p_{jy}, -(p^*_{jx} - p_{jx})]^{\mathrm{T}}$ is the velocity vector perpendicular to the position vector of $p^*_{\alpha j} - p_{\beta j}$.

Theorem 2 Under the control laws of Eq. (8), the β-type follower will rotate around its corresponding α-type one.

Proof Define the following Lyapunov function

$$U = \left(p^*_{\alpha j} - p_{\beta j}\right)^{\mathrm{T}}\left(p^*_{\alpha j} - p_{\beta j}\right) > 0 \tag{9}$$

and differentiating U with respect to time t, we have

$$\begin{aligned}\dot{U} &= 2\left(p^*_{\alpha j} - p_{\beta j}\right)^{\mathrm{T}}\left(\dot{p}^*_{\alpha j} - \dot{p}_{\beta j}\right) \\ &= 2k_1\left(p_{\beta j} - p^*_{\alpha j}\right)^{\mathrm{T}} \\ &\quad \times \left[\left(p^*_{\alpha j} - p_{\beta j} - \frac{p^*_{\alpha j} - p_{\beta j}}{\|p^*_{\alpha j} - p_{\beta j}\|} r^*\right) + \frac{1}{2}\boldsymbol{a}\right] \\ &= 2k_1\left(p_{\beta j} - p^*_{\alpha j}\right)^{\mathrm{T}} \\ &\quad \times \left(\frac{r^* - \|p^*_{\alpha j} - p_{\beta j}\|}{\|p^*_{\alpha j} - p_{\beta j}\|}\left(p_{\beta j} - p^*_{\alpha j}\right) + \frac{1}{2}\boldsymbol{a}\right) \\ &= 2k_1\left(r^* - \|p^*_{\alpha j} - p_{\beta j}\|\right)\|p^*_{\alpha j} - p_{\beta j}\|. \end{aligned} \tag{10}$$

It is obviously to see that when $\|p^*_{\alpha j} - p_{\beta j}\| > r^*$, we can deduce $\dot{U} < 0$. When $\|p^*_{\alpha j} - p_{\beta j}\| = r^*$, we can deduce $\dot{U} = 0$. So the β-type follower will finally keep the safe distance from the α-type one. At the same time, the third term on the right-hand side of Eq. (8) is perpendicular to $p^*_{\alpha j} - p_{\beta j}$, and is not contained in Eq. (10). It is used only to change the motion direction of the β-type follower. So it is easy to deduce that the β-type follower will rotate around its corresponding α-type one with a radius of r^*.

According to Theorem 1 and Theorem 2, it is easy to have the following conclusion.

Corollary 1 Under the control of Eqs. (5) and (8), all β-type followers will move into the leader's interaction range.

Proof It is easy to draw the conclusion from Theorem 1 and Theorem 2, so the proof is omitted.

3.2. Two numbering strategies for minimally persistent graph

In Subsection 3.1, the control laws that make all followers move into the leader's interaction range have been designed. In this section, two numbering strategies to form minimally persistent formation will be presented, of which one is based on relative angles and the other is based on relative distances.

3.2.1. Numbering strategy based on relative angles

The first strategy is designed based on relative angles between the leader and followers. Take the leader as the reference agent, as shown in Fig. 4(a). One can obtain the relative angles θ_i between the leader and followers from the following equation:

$$\theta_i = \begin{cases} \arccos\dfrac{x_i - x_{\mathrm{L}}}{\sqrt{(x_i - x_{\mathrm{L}})^2 + (y_i - y_{\mathrm{L}})^2}}, \\ \quad \text{if } y_i - y_{\mathrm{L}} \geq 0, \\ 2\pi - \arccos\dfrac{x_i - x_{\mathrm{L}}}{\sqrt{(x_i - x_{\mathrm{L}})^2 + (y_i - y_{\mathrm{L}})^2}}, \\ \quad \text{if } y_i - y_{\mathrm{L}} < 0, \end{cases} \quad (i \in \Omega) \tag{11}$$

where $(x_{\mathrm{L}}, y_{\mathrm{L}})$ denotes the position of the leader.

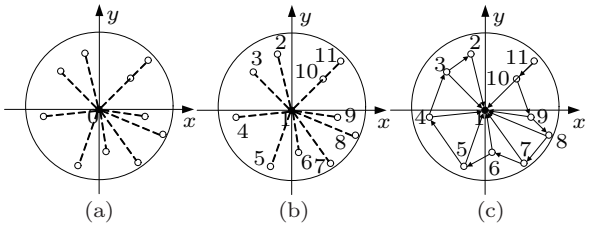


Fig. 4. Leader's interaction ranges denoted by circles. Panel (a) shows the relative positions, panel (b) the numbering process, and panel (c) the minimally persistent graph.

According to the relative angles, the numbering process can be initialized. Then, based on the numbering process, the minimally persistent graph is obtained by adding prescribed directed communication links. The details are as follows.

Step 1 Number the leader as 1. Calculate each angle θ_i between follower i $(i \in \Omega, i \neq 1)$ and the leader by Eq. (11).

Step 2 Choose a follower that is not collinear with another one and the leader as the second follower and number it as 2.

Step 3 Sequence the number of all other followers in a counterclockwise according to their relative angles. If some agents are collinear, then all of these agents are sequenced by relative distances between followers and leader according to the order from small to large. Figure 4(b) shows the process.

Step 4 Set directed communication links from all followers to the leader, as well as from large number followers to small number followers, as shown in Fig. 4(c). The total number of communication links is $2n-3$. The obtained topology graph is a minimally persistent graph.

The above steps are the process to generate minimally persistent graph for the MASs according to their relative angles. Note that, although the angles are utilized here, they are not intended to control the motion of the formation but only to construct the minimally persistent graph.

3.2.2. Numbering strategy based on distances

In Subsection 3.2.1, the first numbering process based on relative angles was presented. But its numbering process is somewhat centralized and the relative positions must be measured. In this section, a second numbering strategy is presented, which is not centralized and only the distances between agents need to be measured.

The leader is also numbered as 1. The next is that all followers move to appropriate positions to keep the desired distance from the leader. The controllers for the followers are presented as follows:

$$u_i = v_0 + k_2 (p_{\mathrm{L}} - p_i)(\|p_{\mathrm{L}} - p_i\| - d_1), \ (i \in \Omega, i \neq 1), \quad (12)$$

where $k_2 > 0$ is a constant. $p_{\mathrm{L}} \in R^2$ denotes the position of the leader, and d_1 the desired distance between followers and the leader.

Theorem 3 Assume that no agents overlap at the initial positions. Then, follower i $(i \in \Omega, i \neq L)$ controlled by Eq. (12) will keep the desired distance d_1 from the leader.

Proof Consider the following equation:

$$e_i(t) = \|p_i(t) - p_{\mathrm{L}}(t)\| - d_1, \ \ (i \in \Omega, i \neq 1).$$

So if we can prove that e_i converge to 0 under Eq. (12), this theorem is proved.

Considering the derivative of e_i with respect to time t, one can obtain from Eq. (12) that

$$\begin{aligned} \dot{e}_i(t) &= \frac{(p_{\mathrm{L}}(t) - p_i(t))^{\mathrm{T}}}{\|p_i(t) - p_{\mathrm{L}}(t)\|} (\dot{p}_{\mathrm{L}}(t) - \dot{p}_i(t)) \\ &= -k_2 \|p_{\mathrm{L}}(t) - p_i(t)\| \cdot e_i(t). \end{aligned}$$

Then one can obtain that

$$e_i(t) = \frac{C\mathrm{e}^{-k_2 \mathrm{d}t} \cdot d_1}{1 - C\mathrm{e}^{-k_2 \mathrm{d}t}}, \ \ C > 0. \quad (13)$$

It is obvious that $e_i(t) \to 0$ when $t \to \infty$, namely, the follower controlled by Eq. (12) will keep the desired distance from the leader.

During the period of motion, collisions between agents should be avoided. The gradient-based method is used in this paper to keep the followers at a safe distance. Let $p_{ij} = \|p_i - p_j\|$ denote the real distance between follower i and follower j. In order to avoid collision and guarantee that no two followers on the same side are collinear with the leader, the controllers are designed as follows:

$$\begin{aligned} u_i^c &= \sum_{j \in N_i} [k_{c2} \boldsymbol{a} \cdot E(p_{ij}) + k_{c1} (p_j - p_i) E(p_{ij})], \\ &\quad (i, j \in \Omega, i \neq j \neq 1), \end{aligned} \quad (14)$$

with

$$E(p_{ij}) = \begin{cases} \dfrac{(p_{ij} - r^*)}{p_{ij}}, & p_{ij} \in (0, r^*], \\ 0, & p_{ij} \in (r^*, \infty), \end{cases}$$

where $r^* > 0$ is the safe distance between agents; k_{c1} and k_{c2} are two positive constants; $\boldsymbol{a} = (p_{jy} - p_{iy}, -(p_{jx} - p_{ix}))^{\mathrm{T}} \cdot \mathrm{sgn}(x_{jx} - x_{ix})$ is the added vector perpendicular to that of $p_j - p_i$.

Theorem 4 Under the control of Eq. (14), collision does not happen between followers and the collinear followers will not be collinear with leader.

Proof The second term on the right-hand side of Eq. (14) is similar to the result of Lemma 3 in Ref. [24]. It is easy to know that it guarantees the collision avoidance. Meanwhile, the first term on the right-hand side of Eq. (14) is an added vector perpendicular to that of $p_j - p_i$. According to Theorem 2, the first term on the right-hand side of Eq. (14) has no influence on collision avoidance, but changes follower's motion direction. So, any two followers who are on the same side and collinear with the leader will not be collinear with the leader any more. Theorem 4 is proved.

In the following, the process of numbering strategy and the generation of minimally persistent graph based on distances are shown in Fig. 5. In the figure, the solid line circle denotes the leader's interaction range while the radius of the dashed line circle denotes the desired distance from the leader. Some detailed steps for the numbering process and the generation of minimally persistent graph are given as follows.

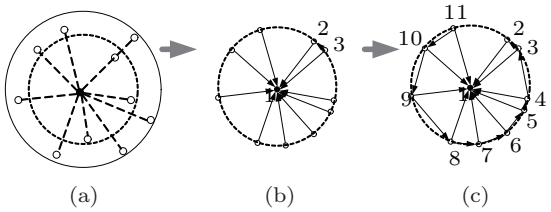


Fig. 5. Process of minimally persistent graph generation based on distances.

Step 1 The leader is numbered as 1. All followers are driven to keep the desired distances from the leader by Eq. (12) as shown in Figs. 5(a) and 5(b).

Step 2 All followers are set to be in direct communication with the leader. Choose anyone as the first follower and number it as 2.

Step 3 Follower 2 finds the nearest neighbor and number it as 3. Then, follower 3 builds a direct communication with follower 2. Figure 5(b) shows the process.

Step 4 For all other neighbors, follower 3 finds the one that satisfies: i) it has a shorter distance from follower 3 than from follower 2. ii) It has the least distance from follower 3. The follower is numbered as 4 and is set to be in direct communication with follower 3.

Step 5 Similar to the analyses of i) and ii) in Step 4, all other followers obtain their numbers by relative distances. Then, agents are set to be in direct communication with followers: from large number followers to small number followers, as shown in Fig. 5(c). The total number of communication links is $2n-3$, and the minimally persistent graph for the MASs is finally obtained.

Now, two methods to generate minimally persistent graphs for the MASs have been presented. The generated topology graphs would keep fixed for the following motion. Compared with the formation control methods requiring the information of all neighbors, the methods proposed in this paper need only $2n-3$ inter-agent communication links and thus reduce the link numbers and communication complexity.

3.3. Control laws for the fixed topology formation

In Subsection 3.2, the fixed topology formation was generated. In order to form a circle formation, the distances between agents must be maintained. For an n-agent persistent formation, there would be $2n-3$ inter-agent distances to be maintained.

The control laws for the generated fixed topology formation are given as follows:

for the leader,

$$u_1 = v_0; \tag{15}$$

for the first follower,

$$u_2 = v_0 + k_2\,(p_{\rm L} - p_2)\,(\|p_{\rm L} - p_2\| - d_1)\,; \tag{16}$$

for the follower that follows another one and the leader,

$$\begin{aligned} u_i \;=\; & v_0 + k_2\,(p_{\rm L} - p_i)\,(\|p_{\rm L} - p_i\| - d_1) \\ & + k_3\,(p_{i-1} - p_i)\,(\|p_{i-1} - p_i\| - d_2)\,, \\ & i \in \{3,4,\ldots,n\}\,, \end{aligned} \tag{17}$$

where k_2 and k_3 are two positive constants; p_i is the position of follower i that follows follower $i-1$; d_1 denotes the desired distance between the leader and follower i; d_2 denotes the desired distance between followers and satisfies that

$$d_2 = 2d_1 \cdot \sin\left(\pi/(n-1)\right)$$

Theorem 5 Under Eqs. (15)–(17), the generated fixed topology formations will converge to a circle formation.

Proof For the proof of Theorem 5, we only need to prove that all followers will move to keep the desired distances under Eqs. (15)–(17).

Firstly, for follower $i=2$ controlled by Eq. (16), it is easy to prove that it will move to keep the desired distance from the leader according to Theorem 3.

Then, we prove that follower $i \in \{3,4,\ldots,n\}$ controlled by Eq. (17) will move to keep the desired distances from both the leader and follower $i-1$.

For follower $i \in \{3,4,\ldots,n\}$ controlled by Eq. (17), it is assumed that its initial relative positions with respect to the leader and follower $i-1$ are shown in Fig. 6(a).

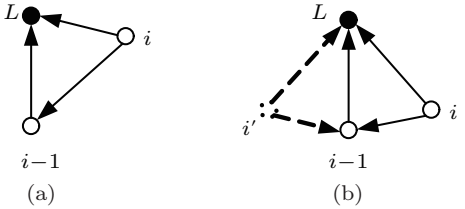


Fig. 6. (a) Initial positions of the three agents and (b) two equilibrium positions.

The input of follower i is described by Eq. (17), which is a vector input. The two basic directions are along the vectors of $\boldsymbol{p}_i\boldsymbol{p}_{\rm L}$ and $\boldsymbol{p}_i\boldsymbol{p}_{i-1}$, respectively. So it can be split into two parts: $u_{i,{\rm L}}$ and $u_{i,i-1}$ without considering the constant velocity v_0, which has no influence on the convergence. For the two parts, $u_{i,{\rm L}} = k_2(p_{\rm L} - p_i)(\|p_{\rm L} - p_i\| - d_1)$ with the reference agent being the leader, and $u_{i,i-1} = k_3(p_{i-1} - p_i)(\|p_{i-1} - p_i\| - d_2)$ with the reference agent being follower $i-1$. The three-agent system is composed of two control parts. The controllers of the two parts are as follows:

Part 1: $\bar{u}_{\rm L} = 0$, $u_{i,{\rm L}} = k_2(p_{\rm L} - p_i)(\|p_{\rm L} - p_i\| - d_1)$;

Part 2: $\bar{u}_{i-1} = 0$, $u_{i,i-1} = k_3(p_{i-1} - p_i)(\|p_{i-1} - p_i\| - d_2)$.

The analyses of the two control parts are similar to those in Theorem 3, it can be proved that $u_{i,i-1}$ and $u_{i,{\rm L}}$ will guarantee the desired distances from follower $i-1$ and the leader, respectively. Follower i will move to the equilibrium position to keep desired distances.

From Eq. (17), it is easy to deduce that there are totally two such equilibrium positions, where follower i keeps both the desired distances, as shown in Fig. 6(b). But because the initial relative position is certain, only the equilibrium position that is on the same side of the initial position is realizable and the other equilibrium position is unrealizable. So, follower i will finally move to the realizable equilibrium position.

Now the convergence of follower $i \in \{3,4,\ldots,n\}$ has been investigated. The stability of follower $i=2$ is also proved by Theorem 3. So, all followers will keep the desired distances. The generated fixed topology formation will converge to a circle formation.

4. Simulation results

In this section, some simulations are provided to illustrate the effectiveness of the proposed methods.

Initially, 13 agents denoted by black points are dispersed in the workplace as shown in Fig. 7(a). Figure 7(b) shows the leader, the α-type followers and the β-type followers. The circle denotes the leader's maximum interaction range. The one in the center is the leader, and the other points in the circle range denote the α-type followers, the remaining points represent the β-type followers. Each β-type follower is set to be in direct communication with its nearest α-type one, indicating that at least one α-type follower is in the interaction range of each β-type follower.

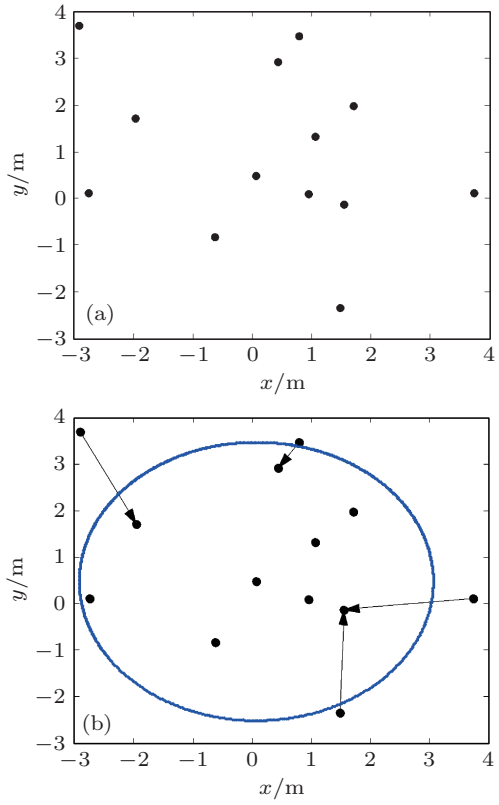


Fig. 7. (color online) Initial dispersed agents.

As for the control of the formation, some parameters are given as follows: $k_1 = k_2 = k_3 = 1$, $k_{c1} = 0.3$, $k_{c2} = 0.1$, $v_0 = [0.3, 0.3]^{\mathrm{T}}$ m/s, $r = 3.0$ m, $r^* = 0.1$ m, and $d_1 = 2$ m. The distance d_2 is calculated to be 1.035 m, i.e., $d_2 = 1.035$ m. The simulation is performed for $t \in [0, 35]$ s.

For the motion of the formation, firstly set $t_1 = 5$ s to displace the β-type followers to guarantee their moving into the leader's interaction range. Figure 8 is the motion trajectories. It can be seen that all the β-type followers move into the leader's interaction range within 5 seconds.

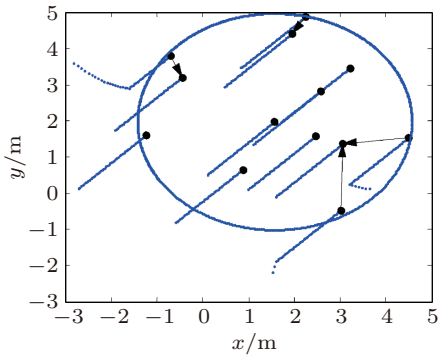


Fig. 8. (color online) Motion of the formation from $t = 0$ s to $t = 5$ s.

4.1. Circle formation based on the first numbering strategy

Since all followers are now in the leader's interaction range, according to Eq. (11) and Steps 1–4 in Subsection 3.2.1, the minimally persistent formation is obtained. Figure 9(a) shows the minimally persistent formation at $t_1 = 5$ s. Then,

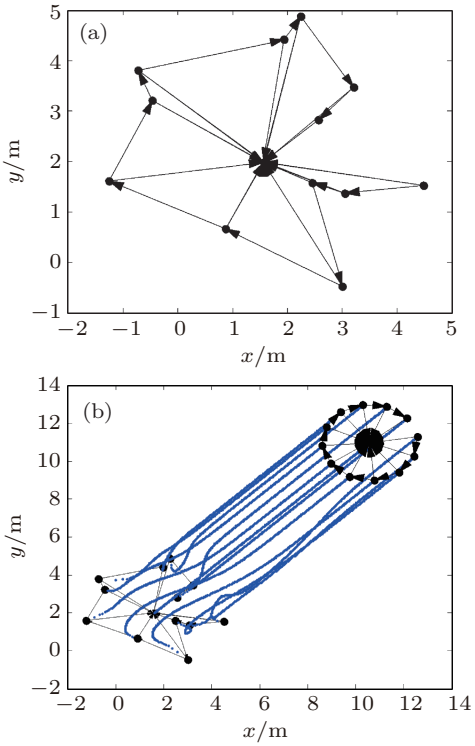


Fig. 9. (color online) Minimally persistent formation and motion trajectories from $t = 5$ s to $t = 35$ s.

controlled by Eqs. (15)–(17), the minimally persistent formation converges to a circle formation. Figure 9(b) shows the motion process from $t = 5$ s to $t = 35$ s. It is obvious from Fig. 9(b) that the fixed topology formation finally reaches a desired uniform circle formation.

To show the results more clearly, the distance errors and velocities of agents are analyzed. Define $e_{\mathrm{L},i} = \|p_i - p_{\mathrm{L}}\| - 2$ as the distance errors between followers and the leader. The results are shown in Fig. 10(a). Define $e_{i,i-1} = \|p_i - p_{i-1}\| - 1.035$ as the distance errors between two neighboring followers, The results are shown in Fig. 10(b). These results show that all errors approximately converge to zero, indicating that all agents are in the desired relative positions. Figure 10(c) shows velocities of agents. One can see that all velocities ultimately converge to the constant v_0.

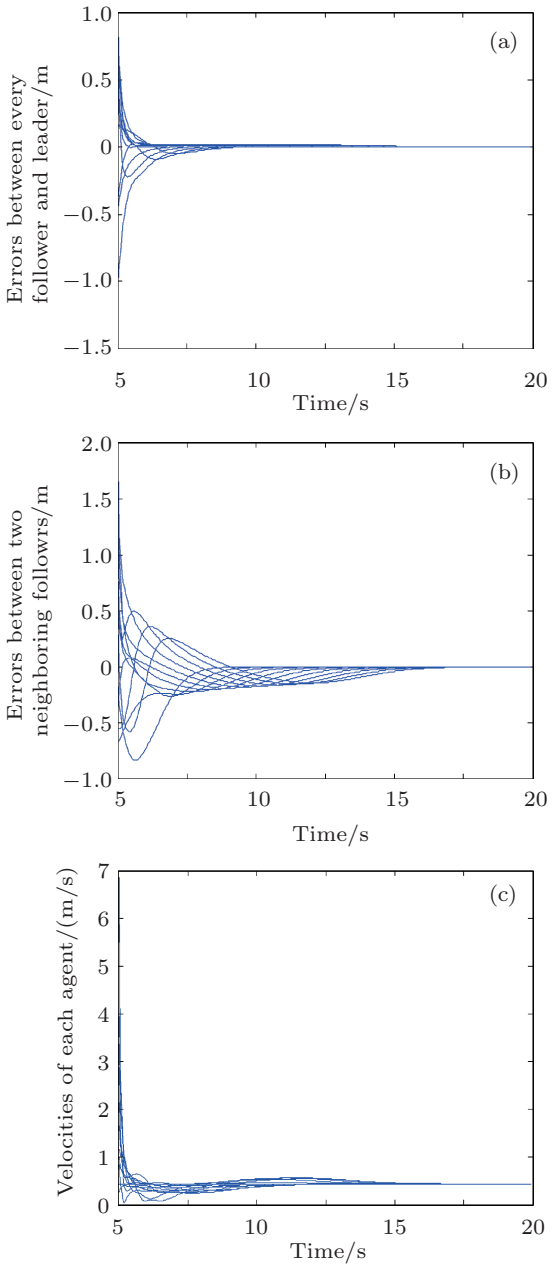


Fig. 10. (color online) Distance errors and velocities of agents.

4.2. Circle formation based on the second numbering strategy

For the second numbering strategy, all followers are firstly displaced to keep the desired distances from the leader. According to Eq. (12) and Theorem 3, the motion process from $t = 5$ s to $t = 15$ s is shown in Fig. 11(a). From the motion trajectories, it is easy to see that all followers succeed in keeping the desired distances. By Steps 1–5 in Subsection 3.2.2, the minimally persistent formation at $t = 15$ s is shown in Fig. 11(b). Figure 11(c) is the motion process from $t = 15$ s to $t = 35$ s under the control of Eqs. (15)–(17). It can be obviously seen that the minimally persistent formation converges to a desired circle formation.

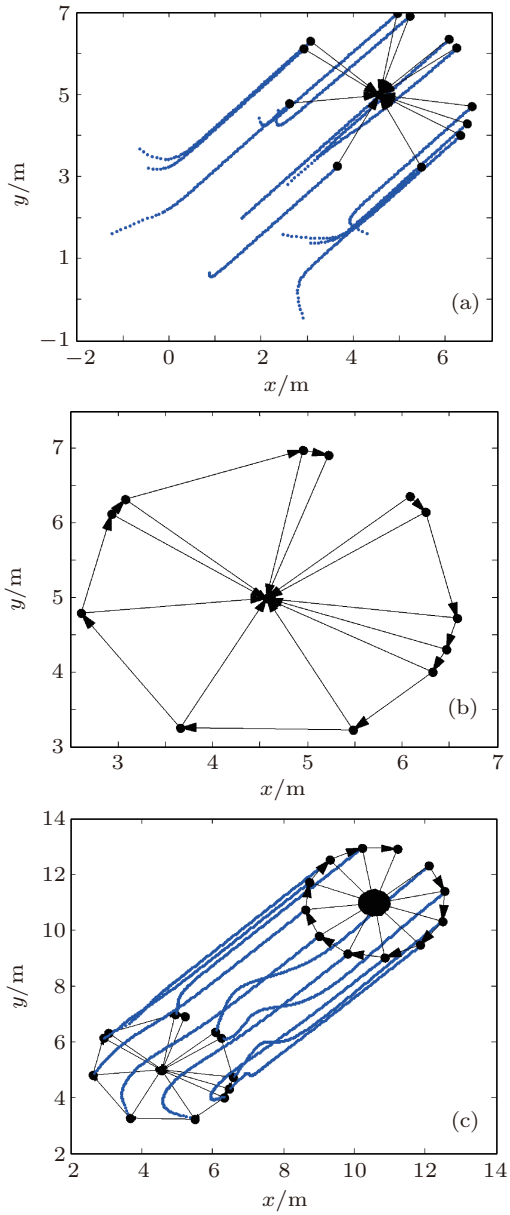


Fig. 11. (color online) Motion of the formation. Panel (a) shows the motion from $t = 5$ s to $t = 15$ s, panel (b) the minimally persistent formation at $t = 15$ s, and panel (c) the motion from $t = 15$ s to $t = 35$ s.

The distance errors and velocities of agents are shown in Fig. 12. Figure 12(a) shows the distance errors between fol-

lowers and the leader. Figure 12(b) shows the distance errors between two neighboring followers. It is obviously seen that all errors converge to zero. The velocities of the agents are shown in Fig. 12(c), from which it can be seen that all velocities converge to the constant v_0.

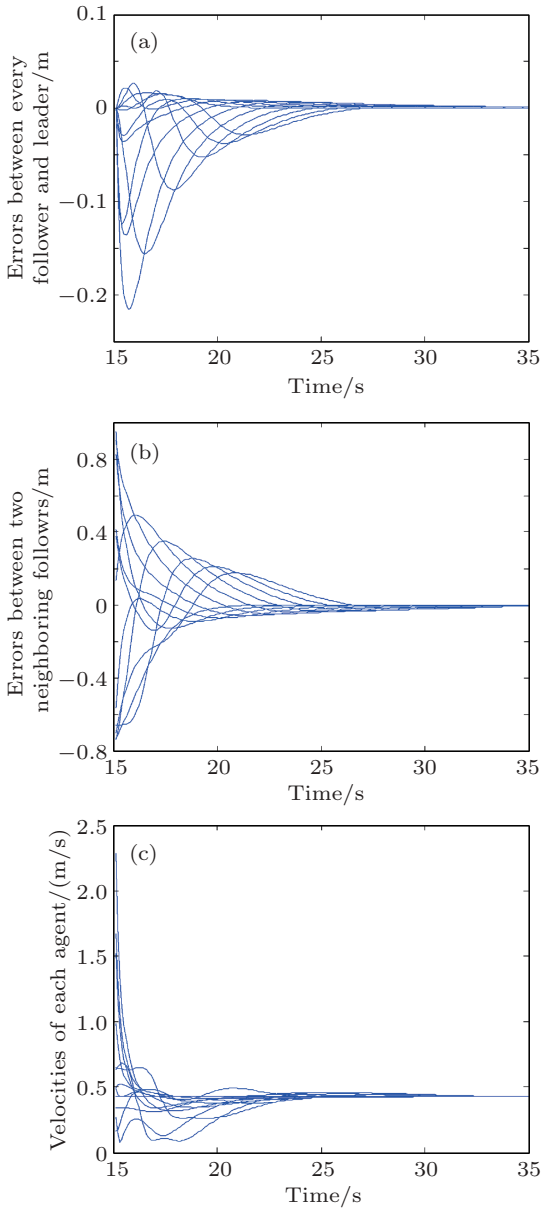


Fig. 12. (color online) Distance errors and velocities of agents.

5. Conclusions

Two numbering strategies for minimally persistent graph generation and controllers design for agents to form circle formation are presented in this paper. Based on the configuration of minimally persistent graph, only $2n-3$ unilateral communication links are needed in the formation control of n agents. The proposed methods in this paper reduce the link numbers and communication complexity. All of the followers are firstly motivated to move into the leader's interaction range. Two numbering strategies based on relative angles and relative distances are presented to form the minimally persistent graphs. Then, gradient-based controllers are designed to form a circle formation while maintaining the desired distances from the corresponding neighbors. Finally, our simulation results illustrate the effectiveness of the proposed numbering strategies and the designed controllers.

As in many practical applications, the time delay between communication agents is an interesting issue for formation control.[24] We may concentrate on studying control laws of time delay in our future work and the results in this paper can also be extended to the case considering time delay.

References

[1] Yuan H and Qu Z 2009 *IET Control Theory & Applications* **3** 712
[2] Cao M, Yu C B and Anderson B D O 2011 *Automatica* **47** 776
[3] Olfati-Saber R 2006 *IEEE Transactions on Automatic Control* **51** 401
[4] Kolling A and Carpin S 2010 *IEEE Transactions on Robotics* **26** 32
[5] Dong W J 2011*Journal of Intelligent & Robotic Systems* **62** 547
[6] Akyildiz I F, Su W, Sankarasubramaniam Y and Cayirci E 2002 *IEEE Commun. Mag.* **40** 102
[7] Balch T and Arkin R C 1998 *IEEE Transactions on Robotics and Automation* **14** 926
[8] Bender J G 1991 *IEEE Transactions on Vehicualr Technology* **40** 82
[9] Swaroop D and Hedrick J K 1999 *ASME Journal of Dynamic Systems, Measurement and Control* **121** 462
[10] Roth B 1981 *American Mathematical Monthly* **88** 6
[11] Smith S, Egerstedt M and Howard A 2009 *Mobile Networks and Applications* **14** 322
[12] Laman G 1970 *J. Eng. Math.* **4** 331
[13] Fidan B, Yu C and Anderson B D O 2007 *IET Control Theory & Applications* **1** 452
[14] Yu C, Hendrickx J M, Fidan B, Anderson B D O and Blondel V D 2007 *Automatica* **43** 387
[15] Hendrickx J M, Fidan B, Yu C B, Anderson B D O and Blondel V D 2008 *IEEE Trans. Autom. Control* **53** 968
[16] Luo X Y, Li S B and Guan X P 2009 *Chin. Phys. B* **18** 3104
[17] Liu T F and Jiang Z P 2013 *Automatica* **49** 592
[18] Cao M, Morse A S, Yu C, Anderson B D O and Dasgupta S 2011 *Communication in Information and Systems* **11** 1
[19] Guo J, Lin Z, Cao M and Yan G 2010 in *Proceedings of American Control Conference*, Baltimore, USA, p. 6822
[20] Guo J, Yan G F and Lin Z Y 2010 *Proceedings of IEEE International Conference on Robotics and Automation*, May 3–8, 2010, Anchorage, USA, p. 1468
[21] Kawakami H and Namerikawa T 2008 *IEEE International Conference on Control Applications*, Sepember 3–5, 2008, San Antonio, USA, p. 1043
[22] Yan J, Luo X Y and Guan X P 2011 *Chin. Phys. B* **20** 018901
[23] Yan J, Luo X Y and Guan X P 2011 *Chin. Phys. B* **20** 048901
[24] Wu J and Shi Y 2011 *Systems & Control Letters* **60** 863